The relationship between global and hemispheric surface temperature averages and the thermohaline circulation

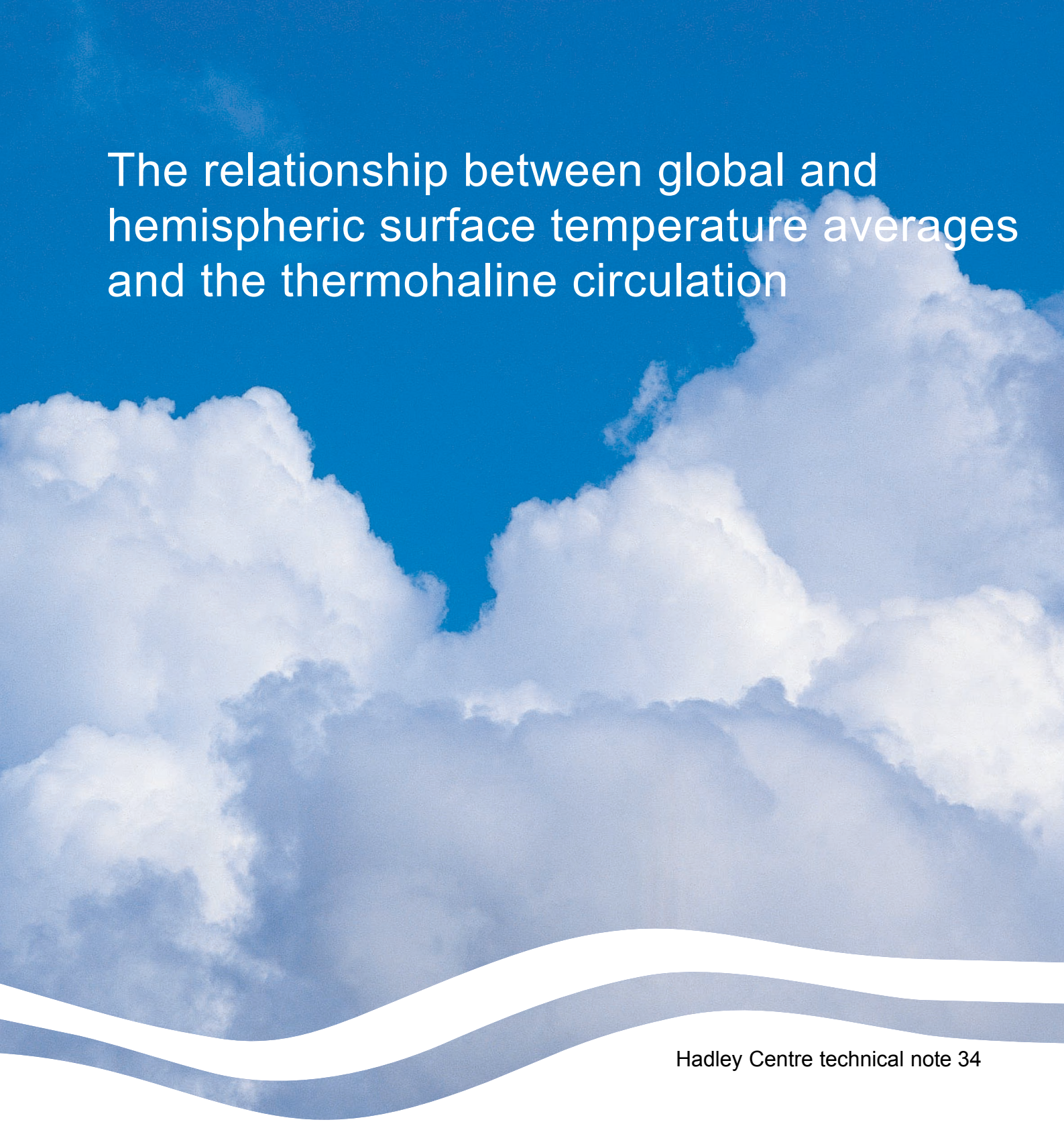

Hadley Centre technical note 34

Jeff Knight, Rob Allan and Chris Folland

December 2001

Met Office

Climate Research Technical Note

The relationship between global and hemispheric surface temperature averages and the thermohaline circulation

Jeff Knight, Rob Allan and Chris Folland

10th December 2001

Abstract

Analysis of a 1400 year coupled climate model calculation without external forcings shows the existence of a quasi-periodic mode of internal climate variability with a characteristic timescale of about 100 years. This mode is manifest in the modelled thermohaline circulation and global and northern hemisphere mean surface temperatures, and has a coherent phase evolution for periods of up to 50 years. It is shown to influence surface temperature in broad regions of the northern hemisphere, particularly in the North Atlantic, Pacific and Asia. In the observed record, both climate change and long period variability act on multi-decadal timescales, hampering identification of either. The model results are used to show that the contribution of the THC-related mode to the observed record of global temperature is potentially significant. In addition, this implies a possible important source of uncertainty in estimating the rate of future climate change.

1. Introduction

Time series of global and hemispheric mean surface temperatures are some of the primary measures of observed climate change. They are useful as indicators of the planetary heat budget free from the variability of local heat transports. Comparisons between model simulations of climate change and observations rely heavily on large scale means for this reason, being much more successful on these rather than smaller spatial scales. Observed climate change is a combination of natural variability, internal to the climate system, as well as transient and secular responses to natural and anthropogenic external influences. The partitioning of these is unclear, however, as secular trends are difficult to isolate from multi-decadal internal variability due the relative shortness of the observational record. This leads to uncertainty in the estimated rate of externally forced climate change. One method of assessing the level of low frequency internal variability is to use a long numerical model simulation without external forcing. In this note results from a 1400 year experiment using the HadCM3 coupled ocean-atmosphere model, are used to show an example of the possible impact of low frequency variability on large scale temperature means.

One potentially important form of internal climate variability is that related to fluctuations in the strength of the thermohaline circulation (THC). The THC is a global mode of oceanic water transport driven by buoyancy differences caused by gradients in ocean temperature and salinity. It involves vertical movement of water, with relatively confined areas of sinking (particularly in the Greenland and Labrador seas) balanced by much broader areas of resurgence. Significant horizontal transports connect these regions. As the oceans are predominantly stably stratified, the THC plays an important part in the recycling of the deep

ocean water with surface water, albeit on timescales of decades to centuries. In the North Atlantic, the THC is responsible for a net northward heat transport which, via the atmosphere, warms the mean surface climate of many parts of the northern hemisphere by several °C (Vellinga and Wood, 2001). Any possible variability in the strength of the THC, therefore, could have important climatic effects. There is, however, insufficient sub-surface marine monitoring to routinely infer the strength of the THC, and so there is no record of possible past fluctuations. As such, we are constrained to use coupled ocean-atmosphere models to make inferences about its potential behaviour. In this note, we examine the relationship between modelled variations in the THC and climate, focussing on the aforementioned large scale surface temperature means. The aim is to test the hypothesis that the magnitude of THC-related variability is significant compared to temperature changes over the observed period.

2. Modelling

The model calculation used is the control run of the third version of the Hadley Centre coupled ocean-atmosphere model, HadCM3 (Gordon *et al.*, 2000). This is a 1400 year integration of the model without any time-varying external forcing, using approximately pre-industrial levels of greenhouse gases. The model is high resolution (3.75° by 2.5°, 19 level atmosphere, 1.25° by 1.25°, 20 level ocean) and requires no adjustment of the heat fluxes at the ocean-atmosphere interface. A full range of physical parameterisations are included consistent with an unsimplified state-of-the-art coupled general circulation model. The climate is realistic and stable, with only a small amount of drift (0.2°C in the global mean surface temperature in 1400 years).

3. Thermohaline Circulation

We take the maximum streamfunction across the Atlantic hydrological section at 30°N as an index of the modelled THC strength. This was chosen as the overall transport is greatest in the North Atlantic, giving a strong signal, yet this latitude is far enough away from the region of sinking to provide a measure of the global circulation. The calculation of different indices by the same method at other latitudes and by different methods has little effect on the characteristics of the resulting time series. The THC index is shown in fig. 1. The time series (upper panel) has been high-pass filtered, removing variability on timescales greater than about 400 years to eliminate model drift. The mean THC flow is found to be about 16 Sv. This is a comparable magnitude to other models (Timmermann *et al.*, 1998; Delworth and Greatbatch, 2000) within the broad limits of uncertainty and comparability of published THC indices. The peak-to-peak variability of the decadal time series is about 2 Sv, or 10-15% of the mean, which is again broadly similar. It is clear that there is considerable variability on inter-decadal timescales, and this is also demonstrated by the power spectrum of the detrended annual THC timeseries shown in the lower panel. For most of the decadal and longer periods, the THC is consistent at the 95% confidence limits (broken lines) with a first-order autoregressive sequence (solid line), or `red spectrum', where low frequency variations result from the integration of the high frequency variability (Hasslemann, 1976). There is also, however, variance at timescales close to 100 years which is stronger than the upper limit of the 95% confidence interval. This indicates the existence of a preferred period of variability which in some way reflects the physical characteristics of the THC, and may represent a fully coupled mode of atmosphere-ocean variability. Support for the reality of this period comes

from a 1000 year control integration of the GFDL coupled model which shows a significant spectral peak between about 70-100 years (Delworth and Greatbatch, 2000). Additionally, a 700 year calculation in the ECHAM3-LSG coupled model (Timmermann *et al.*, 1998) shows a strong concentration of centennial spectral power as well as other peaks.

The enhanced centennial variability in the model suggests that there could be coherent phases of evolution of THC strength. Fig. 2 shows the autocorrelation of the decadal mean THC index for leads and lags of up to 150 years. The zero phase-lag peak has a width of 2-3 decades, suggesting some coherence of THC anomalies over this timescale. In addition, there is a statistically significant (at the 95% level denoted by the dashed lines) anticorrelation at leads and lags of about 50 years. Beyond this, however, correlations are not significant. Thus the model THC is cyclic at the 100 year period with coherency limited to about half a cycle. Rather than being random, therefore, the strength of the THC is predisposed to follow a particular course for a number of decades into the future. Low frequency variations of this kind in observed twentieth century climate variables would be hard to distinguish from a secular trend because of the shortness of the period. So if multidecadal THC fluctuations are related to significant atmospheric climate variability, then there could be an implication for assessing uncertainty in climate change. In the next section we will assess the possibility of climate-THC relationships using results from the control model integration.

4. THC Relationships with Global Surface Temperature

The global mean screen level (i.e. about 1.5 m above the level of the ocean or land surface) temperature is the primary model-derived variable used to assess THC-climate connections. Its evolution is shown in fig. 3, both as annual means (grey line) and as decadal means (black lines), high-pass filtered in the same way as the THC in section 3. Comparison of the size of the model's variability with that derived from observations (IPCC, 2001) is difficult due to the strong trends in the latter, but on interannual timescales at least, it seems to be similar (about 0.5°C). The detrended decadal mean THC index anomaly is also plotted (red line). It is immediately apparent that there are temperature excursions that correspond to peaks or troughs in the strength of the THC. The correlation between the decadal THC and temperature timeseries is 0.49, which is statistically significant at the 95% level. This suggests that there is a mode of climate variability, of which THC strength variations are at least part, which has an important influence on the global mean surface temperature in the model. This is also implied by the temperature power spectrum (fig.4, black line), which shows a peak at the level of significance (dashed line) with about a 100 year period, amongst others, reflecting the centennial peak in the THC (red line). The (sqaured) coherence and phase relationships from a cross-spectral analysis is shown in fig.5. At the timescale where significant power is seen in both spectra (about 100 years) the signals show strong coherence. Peak coherence occurs in bands between 70 and 90 years, although the temperature lacks significant power in this range. The phase difference at 100 years shows the THC lagging temperature by about 5 years.

Lead-lag correlations for the decadal THC and global mean temperature time series (fig. 6) show a strong positive peak centered around the instantaneous correlation, with a significant relationship for 2-3 decades around zero lag, similar to the THC itself (fig. 2). Also like the THC, there are statistically significant (95% interval limits shown by dashed lines), albeit slightly weaker, anticorrelations at leads and lags of about 50 years. The overall similarity of fig. 6 to fig. 2 shows further the common signal in the THC and global mean temperature.

Taken together, the two figures indicate that the mean temperature anomaly also has some temporal coherence as it is predisposed to change sign on a 50 year timescale.

To see the magnitude of the model THC-related temperature variability, decadal average global mean surface temperature is plotted against the decadal average THC-index anomaly (fig. 7), with each decade being represented by a single dot. To this the least-squares linear best fit line has been added, along with the 95% margins of uncertainty in the mean as a function of THC anomaly (solid lines). The regression is clearly positive and significant, in agreement with the aforementioned correlation, and is 0.051 ± 0.016°C Sv^{-1}. As the standard deviation of the decadal THC index is about 0.5 Sv, a THC swing from -1 standard deviation to +1 standard deviation would be expected to be associated with rise in decadal global mean temperature of 0.05°C. A more extreme swing, double this size, would raise the strength of the THC from the lower tail to the upper tail of its distribution, and a temperature rise of 0.1°C would be expected. This change is both significant on the scale of the variability in the model and of changes in the observed temperature record of the twentieth century (about 0.6°C).

5. Hemispheric Mean Surface Temperatures

A similar analysis is now presented for the mean surface temperatures in each hemisphere. For the northern hemisphere, the temperature and THC timeseries are shown in fig. 8. It is clear that the decadal temperature variability is larger than for the global mean, and that here there is also frequent correspondence of peaks and troughs in each timeseries. The correlation coefficient is 0.55, moderately greater than before. The temperature power spectrum (fig. 9) appears to have a very similar form for multi-decadal variations as the global power spectrum, except that significance is further enhanced. Clearly the most significant feature in the low frequency part of the northern hemisphere spectrum is the 100 year THC-related peak. Lead-lag correlations (fig. 10) also show very similar results to the global case, with the same in-phase relationship at zero lag and out-of-phase relationship at leads and lags of about 50 years. The linear regression of mean temperature onto THC index anomalies is 0.089 ± 0.023°C Sv^{-1}, which is rather higher than is found globally. In this instance, 1 and 2 standard deviation swings in the THC index would be expected to be associated with changes in northern hemisphere mean temperature of about 0.1 and 0.2°C respectively. Despite larger changes in the northern hemisphere observed record than globally (of order 1°C for 1901-2000), these swings are on a fractionally larger scale.

Southern hemisphere mean surface temperature is shown in fig. 11. In contrast to the global and northern hemisphere results, correspondence with THC index features is hard to detect, and the correlation (0.13) is not significant. The temperature power spectrum (fig.12) has no significant peaks at multi-decadal timescales, and is therefore consistent with a red spectrum of the integrated high frequency variability. There is little significant correlation at other leads or lags (fig.13) and the linear regression coefficient is not significantly different from zero. Thus the influence of variability associated with THC fluctuations is not apparent in the mean southern hemisphere temperature.

Overall, the modelled northern hemispheire mean temperature has similar but stronger statistical relationships with the THC than the global mean temperature, while the southern hemisphere has no significant relationship. It is fair to view the global response, therefore, as a `dilution' of the northern hemisphere effects. In the next section, we will seek to better

localise the surface temperature variability related to the THC.

6. Surface Temperature Patterns

The lead-lag correlation analysis of the mean temperature in the northern hemisphere (where the THC signal is strongest, fig. 10) shows largest correlations when the THC lags temperature by 60 years, at zero lag and when the THC leads by 40 years. Equivalent correlations and significance at each model grid point are shown in fig. 14. Statistical significance is shown as the fractional chance that a particular correlation is consistent with zero. For the instantaneous correlation (middle panels), there are broad positive correlations across most of the northern hemisphere. The strongest signal is seen in the North Atlantic, where the mid-latitude (35-65°N) THC sensitivity is 0.17°C Sv^{-1}, almost twice the northern hemisphere mean. Other strong signals are seen in the eastern North Pacific ocean, in Greenland and the Labrador Sea, the Caribbean, the Mediterranean region and central Asia. A few areas, such as eastern North America, western Arctic Eurasia and the western North Pacific, show a lack of correlation and significance. Consistent with the area-average results, the southern hemisphere has a mix of positive and negative correlations and generally low significance. The correlations offset in time (top and bottom panels) can be jointly described as a similar pattern with reversed sign. The breadth of significance is not as great as at zero lag, but there are similar regions of confidence, particularly in the North Atlantic, North Pacific and the Mediterranean. This shows that the THC mode is coherent in space as well as in time, and has hemispheric effects rather as well as in the North Atlantic. The pattern of response bears considerable similarity to the interhemispheric pattern identified in analyses of observed sea surface temperature by Folland *et al.* (1999) (see also references therein). Although the southern hemisphere is not so clearly out-of-phase with the north in the model, there is a distinct temperature dipole across equator in the Atlantic. These authors estimate an approximate 70 year period for the mode, close to the 100 year timescale found here. The existence of this variability is strongly suggestive of the reality of the modelled mode and the THC variations associated with it.

7. Comparison with the Observational Record

To illustrate the implications of the relationships between the THC and large scale temperature found in sections 4 and 5, let us suppose that the model's representation of the unobserved THC, and its associated climate fluctuations, are realistic both in terms of character and magnitude. In this case, we look for periods of the model calculation showing similarity with the observed climate record, taken from the a quasi-globally reconstructed version of HadCRUTv (Jones *et al.*, 2001), which contains data for both the land and ocean surface, and which spans the period 1871-present. As the model shows a strong coherent signal in the North Atlantic, the data are averaged after removing the first empirical orthogonal function (EOF; to account for the observed trend) for the basin-wide area in the latitude range 10-70°N. This is band-pass filtered to retain variability on timescales of about 70 years, the apparent approximate period of variations in the data. The same average is computed for the full model calculation and band-pass filtered for timescales of about 100 years. As the model's spectral peak is at about 90 years, the model timeseries is interpolated so that all the timescales in the signal are transformed to 0.8 of their original value. This matches the frequency of the peak signal in the model with the 70 year timescale in the data more closely. The filtered observed timeseries is then correlated with sub-sections of the

transformed model series of the same length, starting each year that allows a full comparison with the data. High correlations for a few periods identify periods where the timeseries from the model and the data are similar, and so perhaps where the THC and North Atlantic climate anomalies might be similar. The best three matching sub-sections are shown in fig. 15. The model period 2902-3066 (164 years length due to the transformation by the model results by a factor of 0.8), is best of all, with a correlation of 0.99, albeit with a rather small number of degrees of freedom. The other sections correlate less well, but are still very similar to the data.

To compare the modelled and observed periods further, fig. 16 shows the global HadCRUTv data along with screen level temperature from the model, band-pass filtered and transformed as for the North Atlantic average, in three extreme decades. These represent a snapshot of the extreme conditions due to the band-pass filtering, and correspond to the observed minimum in the decade 1910-20 (cold), maximum in 1940-50 (warm) and minimum in 1970-80 (cold). The model results are summarised as means of the three realisations of the extreme epochs. Both model and data are expressed as a fraction of the local standard deviation of the band-passed filtered standard deviation. As would be expected using the above method to select the periods for comparison, there is broad agreement in the north Atlantic region, with consistent anomalies between 1 and 2 standard deviations in both data and the model results. The South Atlantic broadly shows a temperature response that is out of phase with the North Atlantic. Western Europe seems to vary in phase with the adjacent Atlantic ocean, as does most of North America. Elsewhere, parallels are harder to identify. For example, the behaviour of the model over Asia and the Pacific appears to have little similarity to the observations. Overall, there is a fairly strong suggestion that temperature in the Atlantic sector (as well as in the large scale means) can be reconstructed using the model periods, but that local patterns away from this region are not reproduced. This is also confirmed by the spread of results from the individual segments (not shown). Significantly, the modelled THC has almost the same phase as the North Atlantic temperature index in each of these three periods (also not shown), suggesting that it is also a robust feature of the Atlantic variability.

It is perhaps not unexpected that the patterns derived from the statistical analysis over the full 1400 years of the model results (fig. 14) are not fully apparent in these shorter segments. Much of the internal variability not related to the THC, especially that known to emanate from the Pacific region, is averaged out over the longer time. In addition, the observed temperatures will certainly be influenced by other factors still, such as volcanic eruptions, solar activity and changing greenhouse gases, despite the attempts to reduce their influence by removing trends. Nevertheless, our ability to find these model segments shows that important features of the climate variability of the observed era are consistent with the THC-climate relationships found in the model.

Conclusions

We have used results from the 1400 year control calculation of the HadCM3 coupled climate model to analyse multi-decadal internal variability. A potentially important part of this variability are fluctuations in the THC, which is responsible for significant global heat transport. A proxy for the THC has been calculated and shows that the model is broadly in agreement with the mean strength and variance of the THC in other coupled climate models. A further feature in common with these models is the existence of a significant spectral peak in the variance of the THC at near centennial periods. It has been shown that this is associated with coherent phases of the THC over several decades. Similar analysis for modelled global

and northern hemisphere mean screen level temperature time series shows a strong relationship between temperature and the THC, with similar centennial peaks in variability. A tendency for opposite anomalies to occur 50 years before and after extrema of decadal temperature has been shown as part of this. For the modelled northern hemisphere mean temperature, a regression of 0.09°C Sv^{-1} is found, implying potential THC-related changes of several tenths of a degree, with even greater sensitivity (0.17°C Sv^{-1}) in the mid-latitude North Atlantic. No such behaviour has been detected in the analysis of southern hemisphere mean temperature. The global results are therefore consistent with a simple `dilution' of the northern hemisphere effects. The geographical pattern of THC-temperature correlations shows broad connections over most of the northern hemisphere, especially in the eastern Atlantic and Pacific and over Asia. We conclude that there is a quasi-periodic mode of model variability involving both the THC and northern hemisphere surface temperature which has some coherency for about half of its roughly 100 year cycle.

The lack of an observed record of the THC prevents validation of its modelled variability. Additionally, the relative shortness of the era of reliable global observations and the strong warming trend make the modelled surface temperature variability difficult to verify. Despite this, encouraging agreement is found with observational analyses by Folland *et al.* (1999), who show a pattern of temperature variability with a similar distribution and period to that seen here. Given the difficulty of characterising this mode in the real climate system, however, we are constrained to use the model results to assess its potential impact. This has been done by comparing an area average of observed North Atlantic SST with a similar average for equivalent length periods of the model calculation. After band-pass filtering and matching the periods of the principle variations in the model and data, three model periods where found in which this North Atlantic index showed a very good agreement with that derived from observations. The ability of the model to produce these periods of similarity and the consistency of the THC timeseries in each case lends weight to the idea that observed variations are related to THC fluctuations, at least in the North Atlantic. Elsewhere, patterns of variability are less consistent between model and data, and between each of the model segments, even though the South Atlantic appears to be out of phase with the North. Making definite conclusions about these relatively short sub-periods is likely to be difficult, however, as there is a substantial amount of low frequency variability in the model that is unrelated to the THC. Despite this, the THC-climate connections found in the model provide a very credible interpretation of observed climate history over large parts of the earth. This has implications for assessments of the rate of future climate change, which may in part depend on future multi-decadal fluctuations of the THC. Our results suggest that this would particularly affect temperature over western Europe, as well as the global and northern hemisphere means.

Acknowledgements

We would like to acknowledge Michael Vellinga who supplied the THC index time series and participated in useful discussions.

References

Delworth, T. L. and R. J. Greatbatch, `Multidecadal thermohaline circulation variability driven by atmospheric surface flux forcing', *J. Climate*, **13**, 1481-1495, 2000.

Folland, C. K., D. E. Parker, A. W. Colman and R. Washington, `Large scale modes of ocean surface temperature since the Late Nineteenth century', in *Beyond El Nino: Decadal and Interdecadal Climate Variability*, Ed: Navarra, A., Springer-Verlag press, Berlin, Germany, 374p, 1999.

Folland, C. K., N. A. Rayner, S. J. Brown, T. M. Smith, S. S. Shen, D. E. Parker, I. Macadam, P. D. Jones, R. N. Jones, N. Nicholls and D. M. H. Sexton, `Global temperature change and its uncertainties since 1861', *Geophys. Res. Lett.*, in press, 2001.

Gordon, C., C. Cooper, C. A. Senior, H. Banks, J. M. Gregory, T. C. Johns, J. F. B. Mitchell and R. A. Wood, `The simulation of SST, sea ice extents and ocean heat transports in a version of the Hadley Centre coupled model without flux adjustments', *Clim. Dyn.*, **16**, 147-168, 2001.

Hasselmann, K., `Stochastic climate models. Part I: theory', *Tellus*, **28**, 473-485, 1976.

IPCC, *`Climate Change 2001: The Scientific Basis. Contribution of Working Group I to the third Assessment Report of the Intergovernmental Panel on Climate Change'* Eds: Houghton, J. T., Y. Ding, D. J. Griggs, M. Noguer, P. J. Van der Linden, X. Dai, K. Maskell and C. A. Johnson, Cambridge University Press, Cambridge, United Kingdom, 881p, 2001.

Jones, P. D., T. J. Osborn, K. R. Briffa, C. K. Folland, E. B. Horton, L. V. Alexander, D. E. Parker and N. E. Rayner, `Adjusting sampling density in grid box land and ocean surface temperature time series', *J. Geophys. Res.*, **106**, 3371-3380, 2001.

Timmermann, A., M. Latif, R. Voss and A. Grotzner, `Northern hemisphere interdecadal variability: a coupled air-sea mode', *J. Climate*, **11**, 1906-1931, 1998.

Vellinga, M. and R. Wood, `Global climatic impacts of a collapse of the Atlantic thermohaline circulation', submitted to *Climatic Change*, 2001.

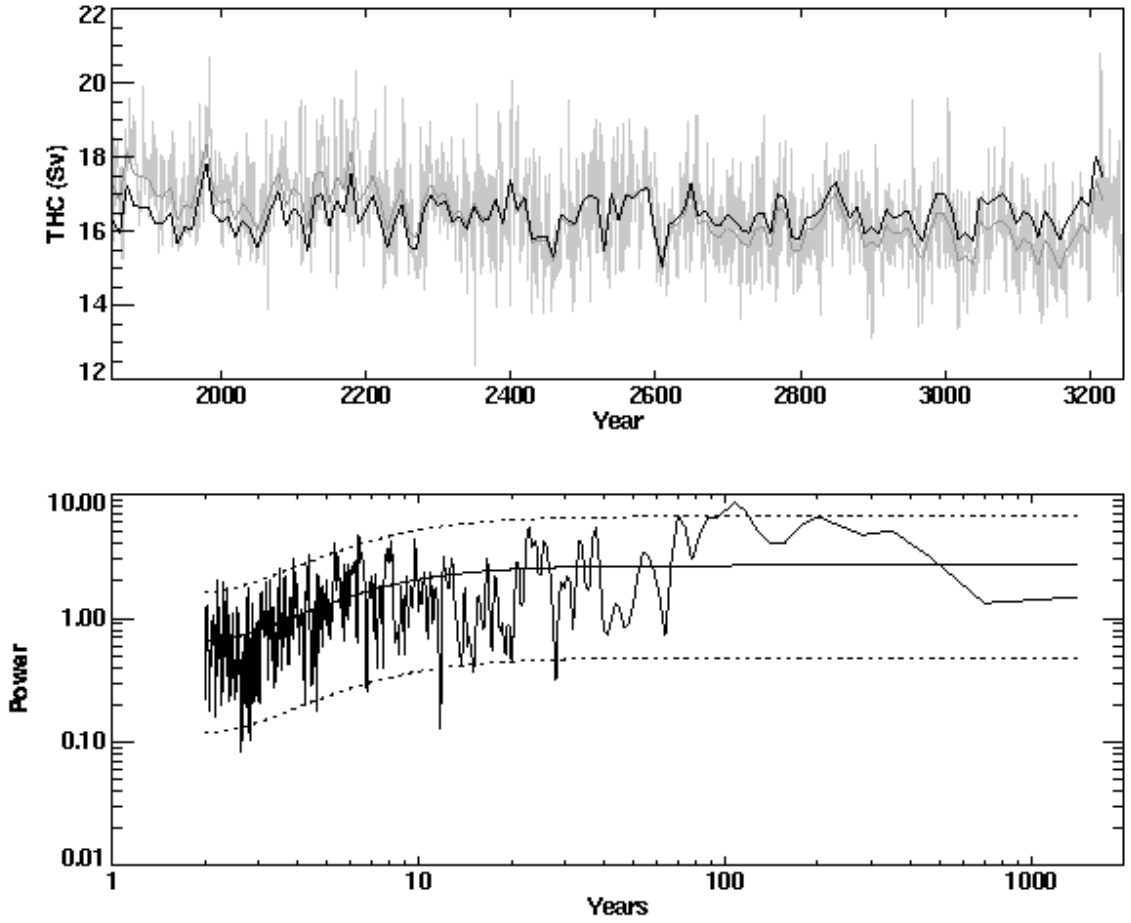

Figure 1. Upper Panel: Evolution of the model THC (defined in the text) in Sverdrups as a function of time in arbitrary years. The grey lines represent the annual averages and the decadal averages overlain. The black line represents the decadal THC index with the model drift removed by using a high-pass filter that eliminates variations on timescales longer than roughly 400 years. Lower Panel: Power spectrum of the annual average THC detrended by removing a least-sqaures linear fit. The smooth solid line is the power of a red noise spectrum with the same AR(1) coefficient as the data and the dashed lines are 95% confidence limits.

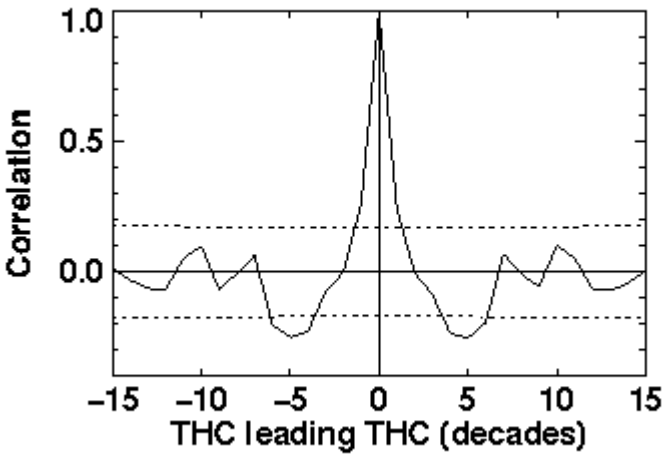

Figure 2. Autocorrelation of the decadal THC index at leads and lags of up to 150 years. Note that the symmetry between leads and lags is expected in this calculation. Dotted lines show the 95% confidence limits for the null hypothesis that the correlation is zero.

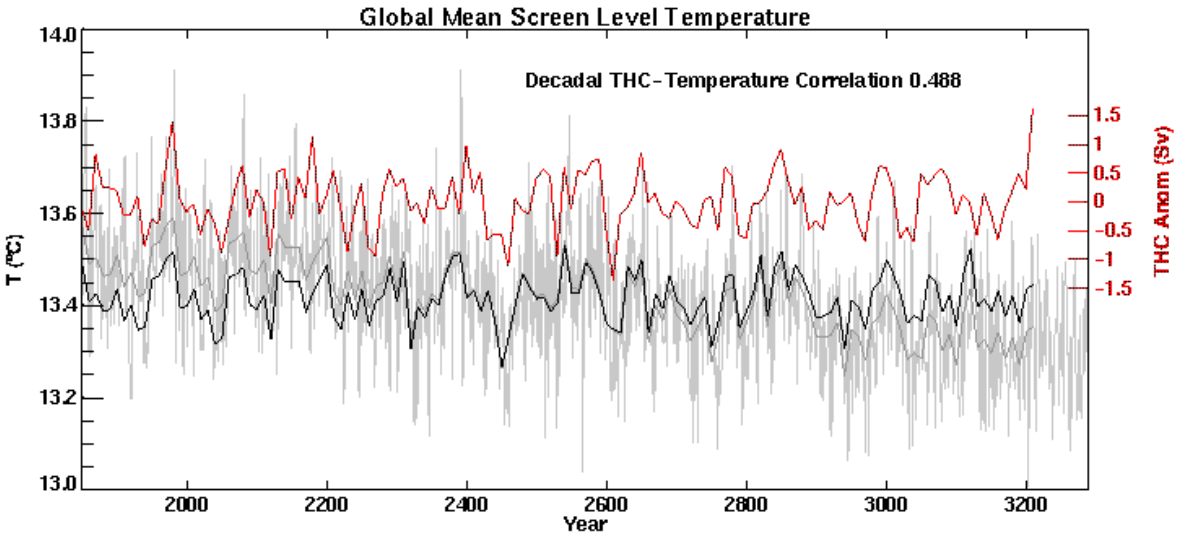

Figure 3. Global mean screen level temperature evolution in the model. The annual time series is plotted in grey, with the decadal mean superimposed. The decadal average, filtered as the THC in fig. 1, is in black. The THC itself is plotted in red for comparison.

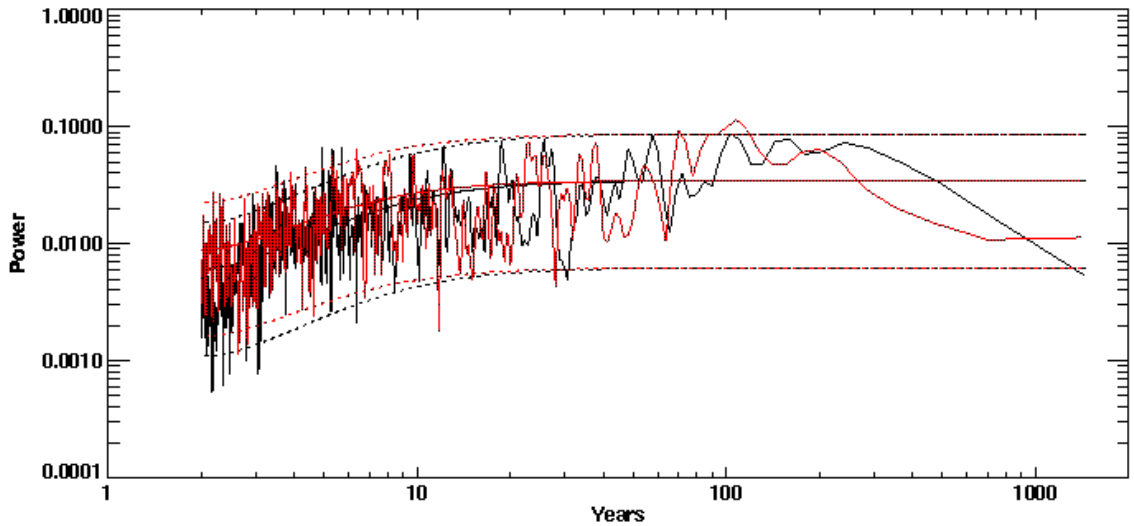

Figure 4. Power spectrum of the detrended annual global mean screen temperature (black) compared to the power spectrum of the detrended annual THC (red). The THC spectrum has been scaled for ease of comparison. For each spectrum the red noise spectrum is shown by the smooth continuous lines and the 95% confidence limits by the broken lines.

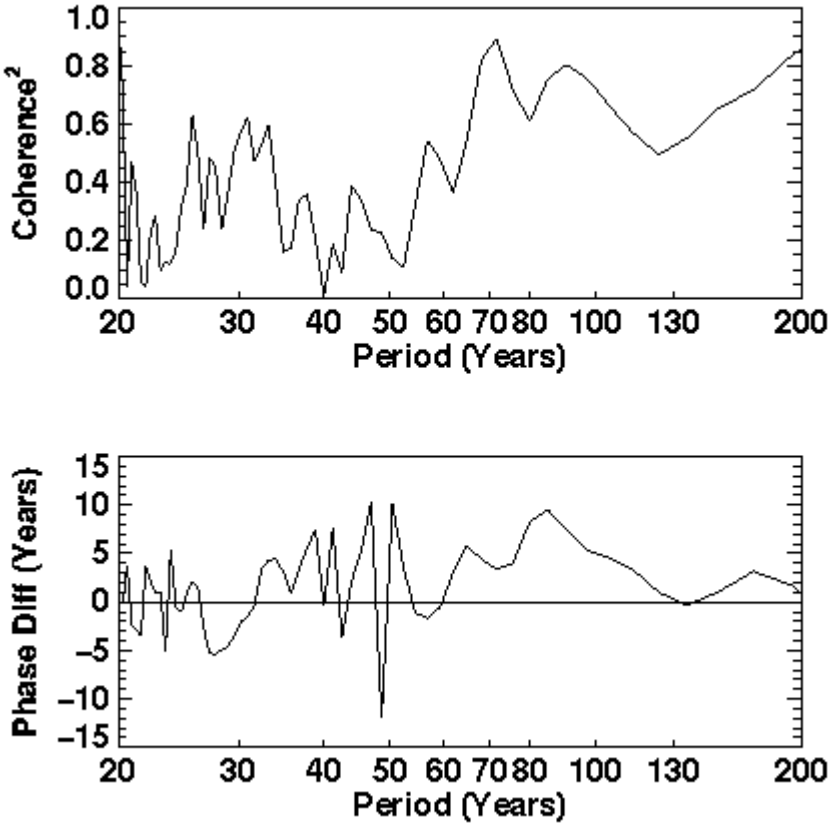

Figure 5. Coherence (sqaured) (upper pannel) and phase difference (expressed in years) (lower panel) from a cross-spectral analysis of the THC index and global mean screen level temperature.

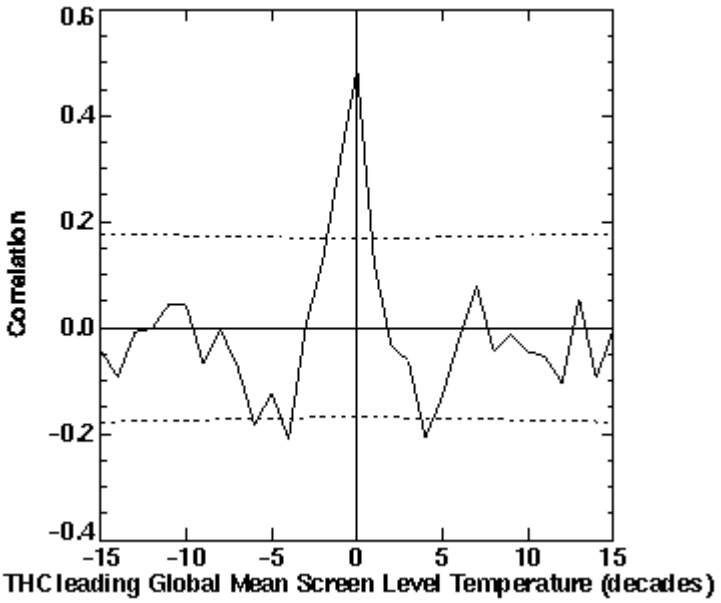

Figure 6. Correlation of the global temperature with the decadal THC index at leads and lags of up to 150 years. For positive times (THC leading) the temperature is compared to the past THC. For negative times (THC lagging) the temperature is compared to the future THC. Dotted lines show the 95% confidence limits for the null hypothesis that the correlation is zero.

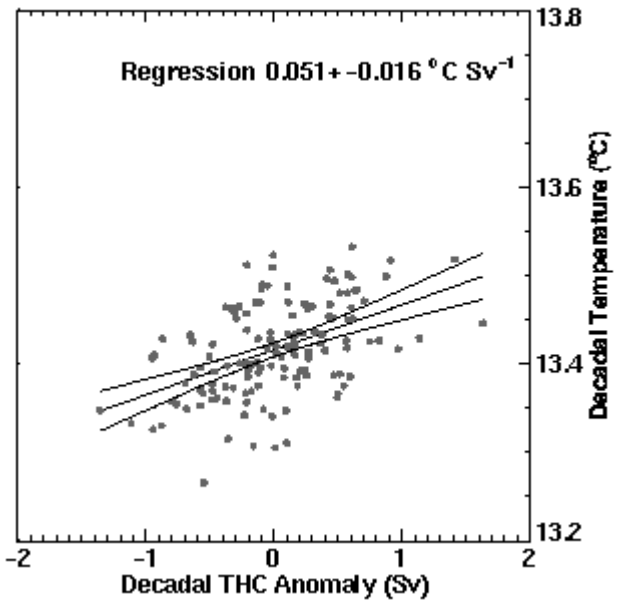

Figure 7. Regression of decadal global temperature against decadal THC anomaly. Each point represents one decade. The best fit linear trend is shown (straight line) along with the 95% confidence interval of the mean temperature as a function of THC anomaly (curves). This gives a graphical measure of the uncertainty in the trend.

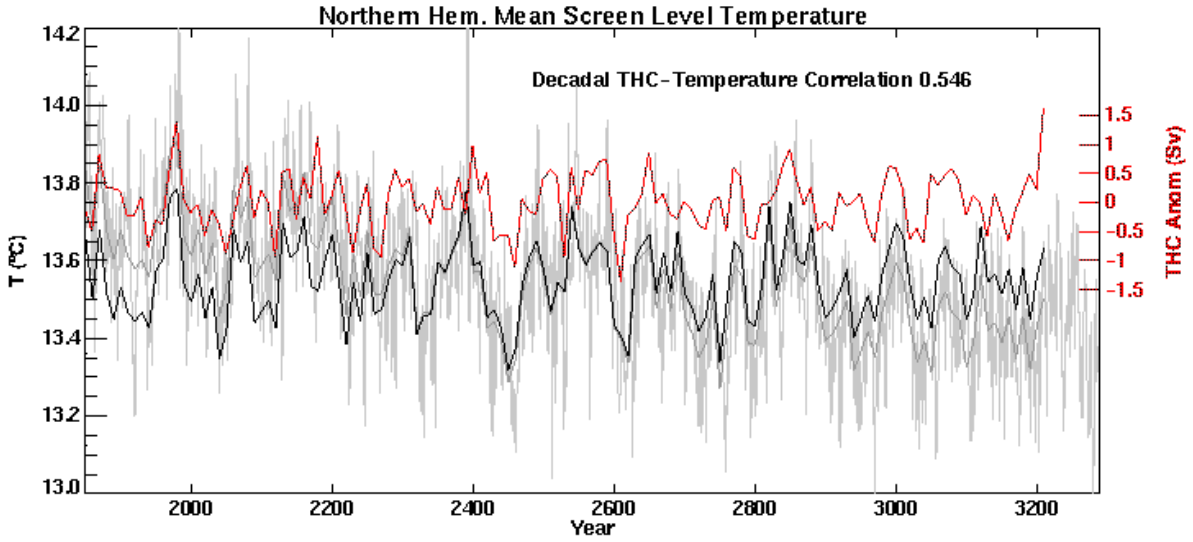

Figure 8. As fig. 3 but for northern hemisphere mean screen level temperature.

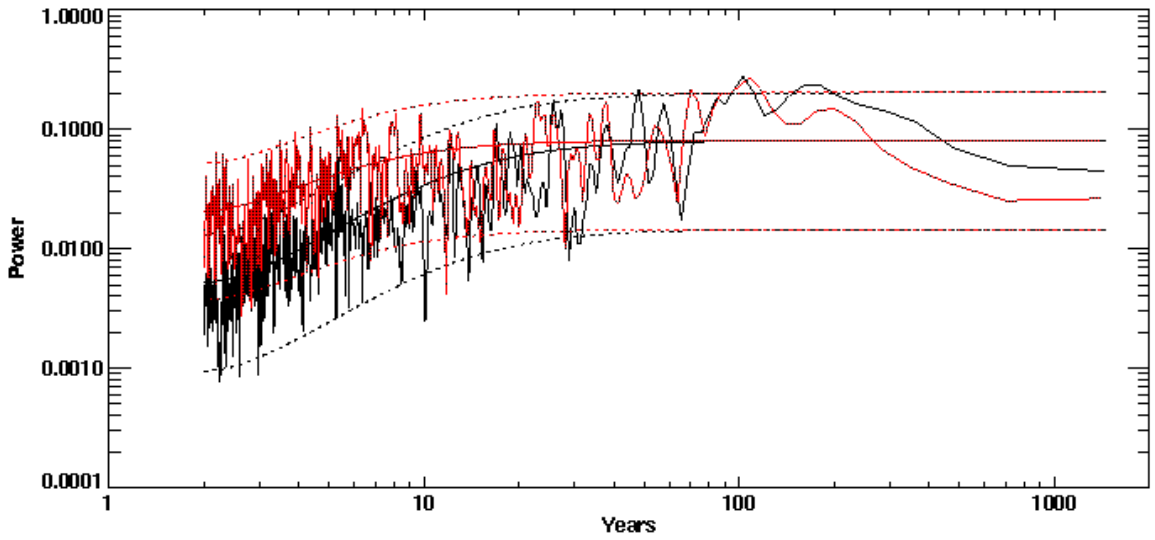

Figure 9. As fig. 4, but for northern hemisphere mean screen temperature (black) and the THC (red).

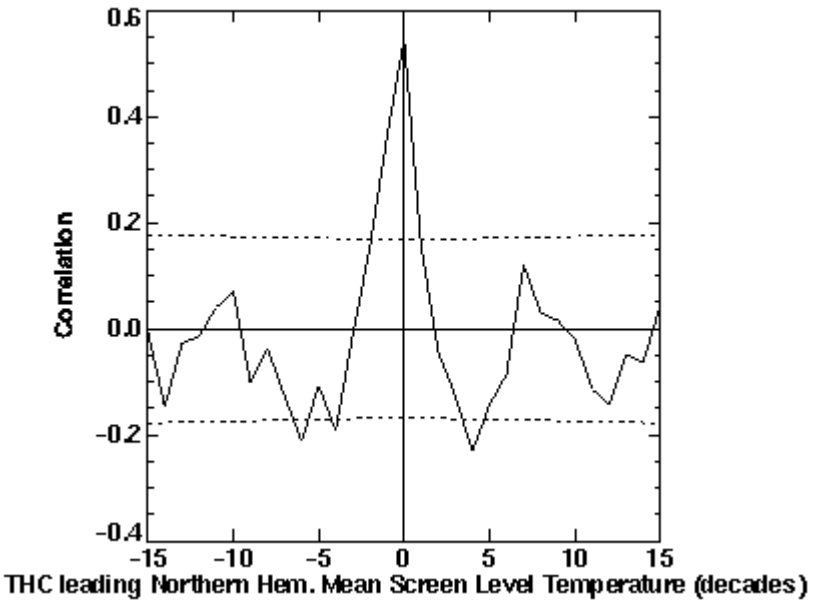

Figure 10. As fig. 6 but for northern hemisphere mean screen temperature.

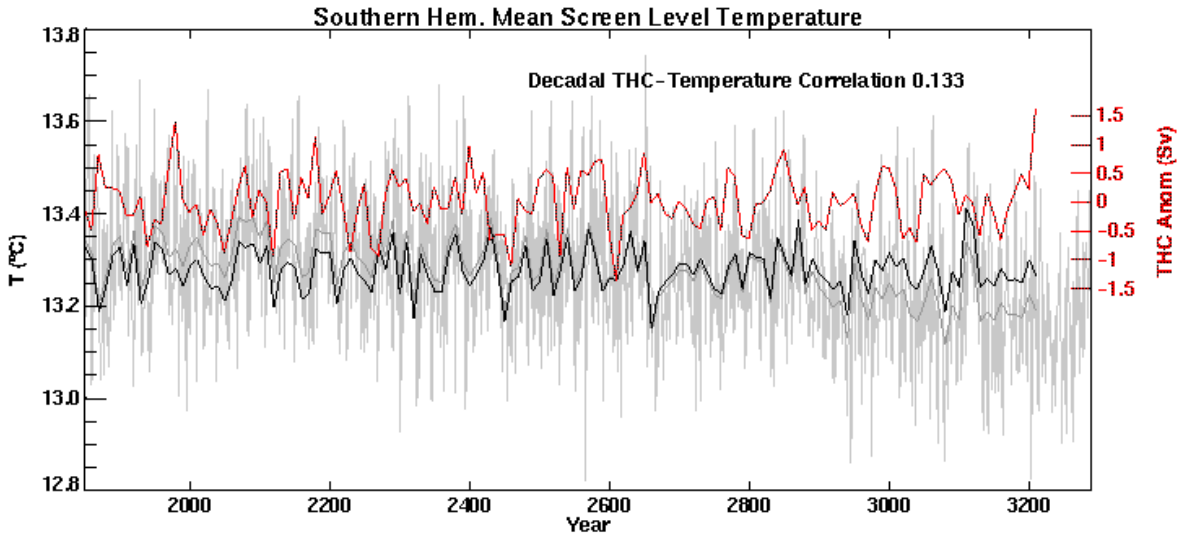

Figure 11. As fig. 3, but for southern hemisphere mean screen level temperature.

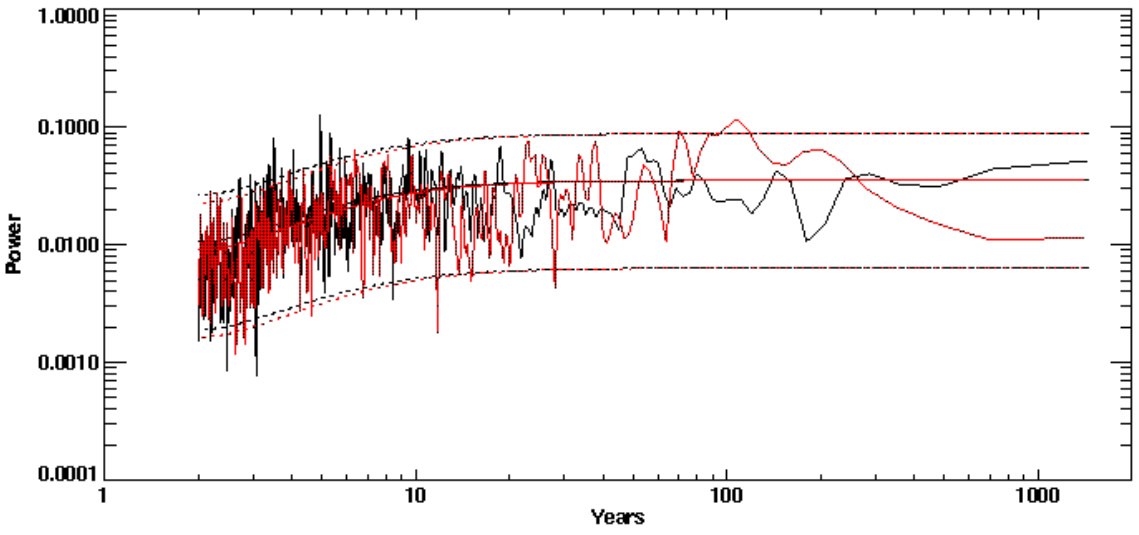

Figure 12. As fig. 4 but for southern hemisphere mean screen temperature (black) and THC (red).

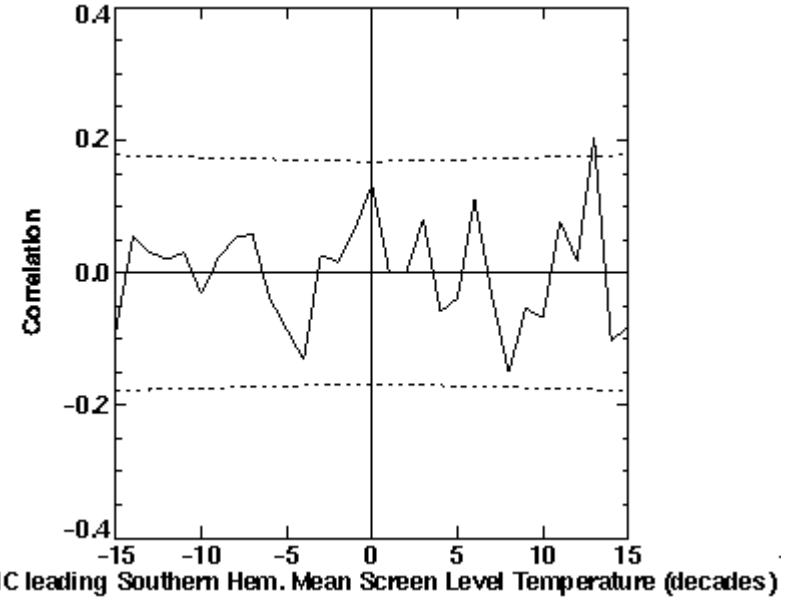

Figure 13. As fig. 6 but for southern hemisphere mean screen level temperature.

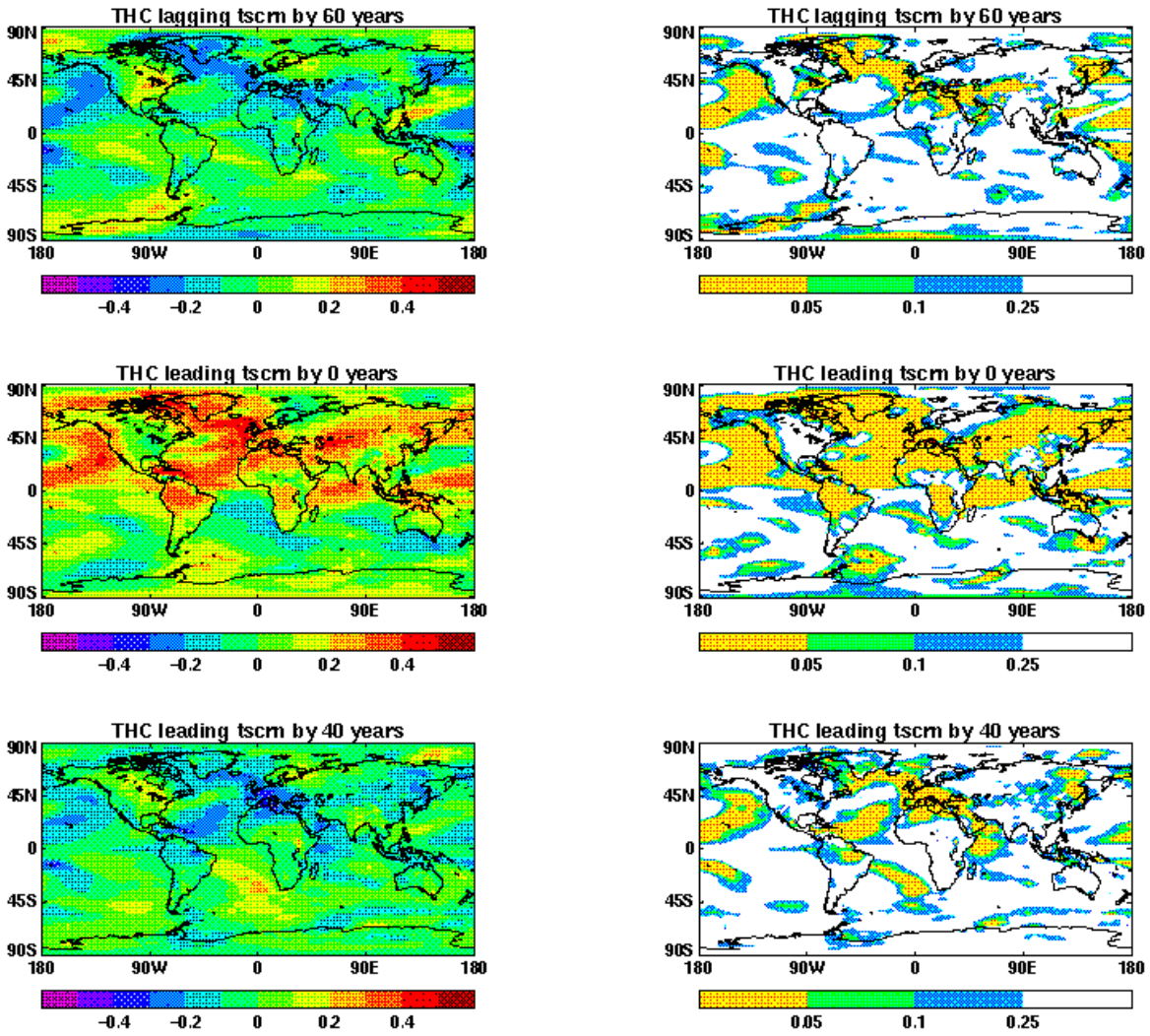

Figure 14. Model grid-point correlations and significance with the THC. The upper panels show the relationship between decadal annual screen level temperature and the decadal annual THC index 60 years later, while the middle panels are for synchronous decadal variations, and the lower panels relate decadal temperature to the decadal THC index 40 years beforehand. The left-hand panels show the spatial variations in correlation and the right-hand panels show the corresponding significance, defined here as the fractional probability that the correlation is zero.

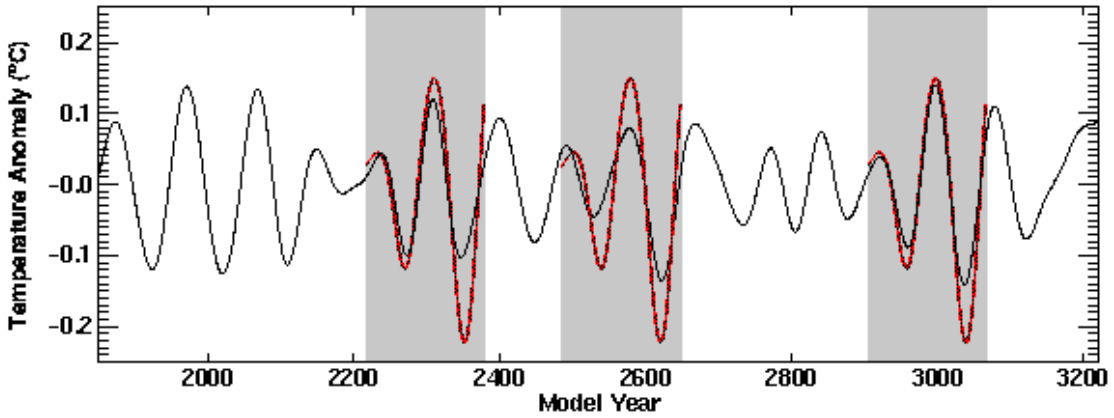

Figure 15. Model North Atlantic avergage sea surface temperature anomalies (see text for deifinition) band-passed filtered to select variations on the 70-130 year timescale (black curve). The band-pass filtered observed North Atlantic average temperature (red curves) are plotted over each of the model segments found to match the data, with these periods highlighted by shading.

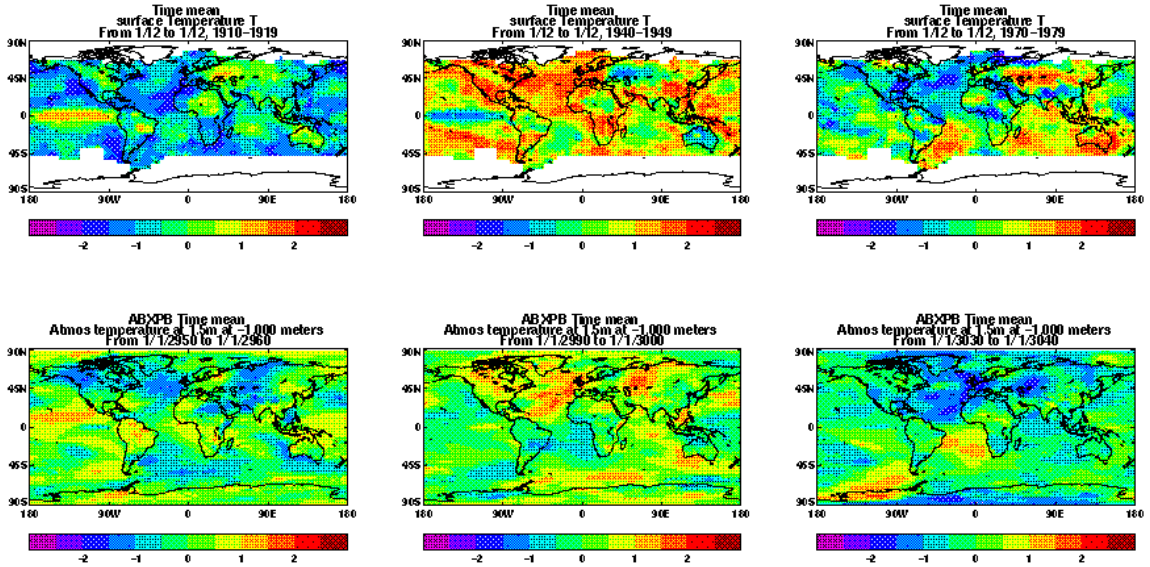

Figure 16. Observed detrended surface temperature (top row) band-pass filtered using a filter centred on 70 years for the epochs of low (1910s - left), high (1940s - centre) and low (1970s - right) North Atlantic sea surface temperatures (SSTs). The average of the three model segments representing surface temperature realisations with similar North Atlantic SST evolution are plotted (bottom row) for equivalent epochs.